AMERICAN ACADEMY OF OPHTHALMOLOGY®

# Magnetic Resonance Imaging Can Reliably Differentiate Optic Nerve Inflammation from Tumor Invasion in Retinoblastoma with Orbital Cellulitis

*Robin W. Jansen, MD,[1,2] Sophie van der Heide, MD,[1] Liesbeth Cardoen, MD,[2,3,4] Selma Sirin, MD, PhD,[2,5] Christiaan M. de Bloeme, MD,[1,2] Paolo Galluzzi, MD,[2,6] Sophia Göricke, MD,[2,5] Hervé J. Brisse, MD, PhD,[2,3,4] Philippe Maeder, MD,[2,7] Saugata Sen, MD,[8] Eva Biewald, MD,[9] Jonas A. Castelijns, MD, PhD,[1,2] Annette C. Moll, MD, PhD,[10] Paul van der Valk, MD, PhD,[11] Marcus C. de Jong, MD, PhD,[1,2] Pim de Graaf, MD, PhD,[1,2] for the European Retinoblastoma Imaging Collaboration**

***Purpose:*** To investigate the prevalence and magnetic resonance imaging (MRI) phenotype of retinoblastoma-associated orbital cellulitis. Additionally, this study aimed to identify postlaminar optic nerve enhancement (PLONE) patterns differentiating between inflammation and tumor invasion.

***Design:*** A monocenter cohort study assessed the prevalence of orbital cellulitis features on MRI in retinoblastoma patients. A multicenter case–control study compared MRI features of the retinoblastoma-associated orbital cellulitis cases with retinoblastoma controls.

***Participants:*** A consecutive retinoblastoma patient cohort of 236 patients (311 eyes) was retrospectively investigated. Subsequently, 30 retinoblastoma cases with orbital cellulitis were compared with 30 matched retinoblastoma controls without cellulitis.

***Methods:*** In the cohort study, retinoblastoma MRI scans were scored on presence of inflammatory features. In the case–control study, MRI scans were scored on intraocular features and PLONE patterns. Postlaminar enhancement patterns were compared with histopathologic assessment of postlaminar tumor invasion. Interreader agreement was assessed, and exact tests with Bonferroni correction were adopted for statistical comparisons.

***Main Outcome Measures:*** Prevalence of retinoblastoma-associated orbital cellulitis on MRI was calculated. Frequency of intraocular MRI features was compared between cases and controls. Sensitivity and specificity of postlaminar optic nerve patterns for detection of postlaminar tumor invasion were assessed.

***Results:*** The MRI prevalence of retinoblastoma-associated orbital cellulitis was 6.8% (16/236). Retinoblastoma with orbital cellulitis showed significantly more tumor necrosis, uveal abnormalities (inflammation, hemorrhage, and necrosis), lens luxation (all $P < 0.001$), and a larger eye size ($P = 0.012$). The inflammatory pattern of optic nerve enhancement (strong enhancement similar to adjacent choroid) was solely found in orbital cellulitis cases, of which none (0/16) showed tumor invasion on histopathology. Invasive pattern enhancement was found in both cases and controls, of which 50% (5/10) showed tumor invasion on histopathology. Considering these different enhancement patterns suggestive for either inflammation or tumor invasion increased specificity for detection of postlaminar tumor invasion in orbital cellulitis cases from 32% (95% confidence interval [CI], 16–52) to 89% (95% CI, 72–98).

***Conclusions:*** Retinoblastoma cases presenting with orbital cellulitis show MRI findings of a larger eye size, extensive tumor necrosis, uveal abnormalities, and lens luxation. Magnetic resonance imaging contrast-enhancement patterns within the postlaminar optic nerve can differentiate between tumor invasion and inflammatory changes. *Ophthalmology 2022;129:1275-1286* © *2022 by the American Academy of Ophthalmology. This is an open access article under the CC BY license (http://creativecommons.org/licenses/by/4.0/).*

*Supplemental material available at www.aaojournal.org.*

Retinoblastoma is an oncologic disease of the developing retina, typically presenting in patients younger than 5 years of age. Retinoblastoma occurs in a heritable form (40% of cases, mostly bilateral) and a nonheritable form (60% of cases, always unilateral). Mortality ranges from < 5% in high-income countries to 40% to 70% in low-income countries.[1] Survival is poor in the presence of central nervous system metastases.[2] Histopathological postlaminar optic nerve invasion (PLONI) of the tumor is a risk factor for developing metastatic disease. Optic nerve invasion can be detected on magnetic resonance



https://doi.org/10.1016/j.ophtha.2022.06.013
ISSN 0161-6420/22

imaging (MRI) as contrast enhancement in the optic nerve beyond the lamina cribrosa: postlaminar optic nerve enhancement (PLONE).[3-5] Sporadically, in patients with extensive PLONI, a profound thickening of the nerve can be present.[6] Magnetic resonance imaging–based risk stratification is increasingly important as emerging eye-sparing treatments diminish the availability of histopathologic material.[7,8] Interpretation of PLONE on MRI aids clinical decision making regarding enucleation versus conservative (eye-sparing) treatment and refinements of these treatment regimens, for example, to add neoadjuvant chemotherapy or to perform an extended dissection of the optic nerve in case of enucleation.[6,9]

In case of retinoblastoma-associated orbital cellulitis, metastatic risk factor assessment may be complicated because of extensive sterile inflammation within the orbit.[10,11] The clinical presentation with orbital cellulitis has been reported in approximately 5% of retinoblastoma patients.[11-13] Orbital cellulitis can be a presenting feature or can develop during treatment or follow-up. Clinical symptoms include soft tissue swelling, conjunctival chemosis and hyperemia, uveitis, rubeosis iridis, increased intraocular pressure, and increased eye size (buphthalmos).[10,11,14,15] The inflammation in retinoblastoma-associated orbital cellulitis is not infectious (i.e., bacterial or viral) but is probably caused by the tumor outgrowing its local blood supply or suppressing the central retinal artery, leading to auto-infarction and necrosis with necrotic products causing sterile inflammation.[11] Retinoblastoma-associated orbital cellulitis has been described in case reports and in small case series as advanced stage cases with extensive tumor necrosis on histopathologic examination.[11,15-19] One small case series and one case report described MRI characteristics of retinoblastoma-associated orbital cellulitis showing large tumors with necrosis, peritumoral inflammation, lens luxation, and a strong contrast enhancement of the choroid indicating uveitis.[10,17] Contrast enhancement in the distal optic nerve was present (PLONE) in some of these children, suggesting the presence of PLONI, which turned out to be a false-positive finding after enucleation.[10,17]

The hypothesis of this study is that, in patients with retinoblastoma-associated orbital cellulitis, the inflammation itself may cause PLONE on MRI, falsely suggesting tumor invasion and an increased metastatic risk. The purpose of this study was to investigate the MRI prevalence of retinoblastoma-associated orbital cellulitis and to assess concomitant intraocular MRI features. Furthermore, this study aimed to assess sensitivity and specificity of PLONE for predicting PLONI in retinoblastoma with orbital cellulitis. Finally, this study aimed to identify specific optic nerve enhancement patterns differentiating between inflammation and tumor invasion.

## Methods

### Study Design and Patient Samples

This combined retrospective consecutive cohort and retrospective case–control study is reported in accordance with the Standards for Reporting of Diagnostic Accuracy Studies 2015 guidelines.[20] Institutional review board/ethics committee approval was obtained with waiver of informed consent. The study adhered to the tenets of the Declaration of Helsinki. This study consisted of 2 parts: part I is a retrospective cohort study assessing prevalence of retinoblastoma-associated orbital cellulitis on MRI. A consecutive cohort of retinoblastoma patients from January 1995 to November 2020 from a single institution was screened. Figure 1 (part I) shows the patient sample selection of part I. Patients were included if a pretreatment MRI was available, including at least T2-weighted, T1-weighted, and contrast-enhanced T1-weighted sequences. In part II, a case–control study, retinoblastoma cases with orbital cellulitis from part I were included, supplemented with orbital cellulitis retinoblastoma cases from 5 tertiary retinoblastoma referral centers selected by convenience sampling and matched controls (Fig 1, part II). In case of orbital cellulitis on MRI, the ophthalmic records were screened for the presence of a clinical diagnosis of orbital cellulitis. Controls without orbital cellulitis were matched on the basis of availability of histopathology, age at diagnosis, and scan date. At random, a minimum of 10 cases of histopathological proven PLONI were selected. Subsequently, the diagnostic accuracy of PLONE for predicting PLONI in the context of orbital cellulitis was analyzed by comparison with histopathologic results.

### MRI Assessment

**Part I: Screening on Orbital Cellulitis.** Magnetic resonance imaging scans were scored on the presence of orbital inflammation features: (1) preseptal inflammation (fat infiltration, swelling, and enhancement of the eyelid); (2) proptosis (abnormal forward displacement of the globe, comparing the posterior ocular wall with the position of the contralateral eye); (3) postseptal inflammation (fat infiltration and enhancement of postseptal/extraconal fat); (4) swelling and enhancement of extraocular muscles; and (5) swelling and enlargement of the lacrimal gland (dacryoadenitis). Images were scored independently by 2 readers (R.W.J. and P.d.G., with 4 and 15 years of experience, respectively, in ocular MRI). Orbital cellulitis was diagnosed in case of $\geq$2 positively scored inflammation features. In case of disagreement, agreement was reached by consensus.

**Part II: Intraocular Features and Metastatic Risk Factors.** Magnetic resonance images of retinoblastoma-associated orbital cellulitis and controls were scored on 16 items of the validated "Retinoblastoma Imaging Atlas,"[21] supplemented with 5 inflammation features (part I) and the presence of PLONE and optic nerve enlargement. All features were qualitatively assessed, except for tumor volume (quantitative after manual tumor segmentation). In case of PLONE, PLONE patterns were scored. We defined an inflammatory and tumor-invasive PLONE pattern through expert opinion and discussion within the European Retinoblastoma Imaging Collaboration before performing scoring. Inflammatory PLONE was defined as an enhancement equal to or greater in signal intensity compared with choroidal enhancement in a rectangular shape covering the whole superficial width of the lamina cribrosa and distal optic nerve (Fig 2A). Tumor-invasive PLONE was defined as an enhancement pattern with an enhancement less intense than choroidal enhancement in a triangular shape into the optic nerve (Fig 2B, reuse of previously published images in different context with permission of the publisher[22]). In case of presence of both enhancement patterns, cases were considered as being tumor-invasive PLONE in further analyses. The scoring was performed independently by 2 readers (P.d.G. and M.d.J., with 15 and 9 years of experience, respectively, in ocular MRI). The readers were blinded for study group (cases/controls) and clinical information. In case of disagreement between the 2 readers, agreement was reached by consensus. For PLONE on MRI, agreement between study read and clinical read was also assessed. Histopathological data were scored on the presence of PLONI

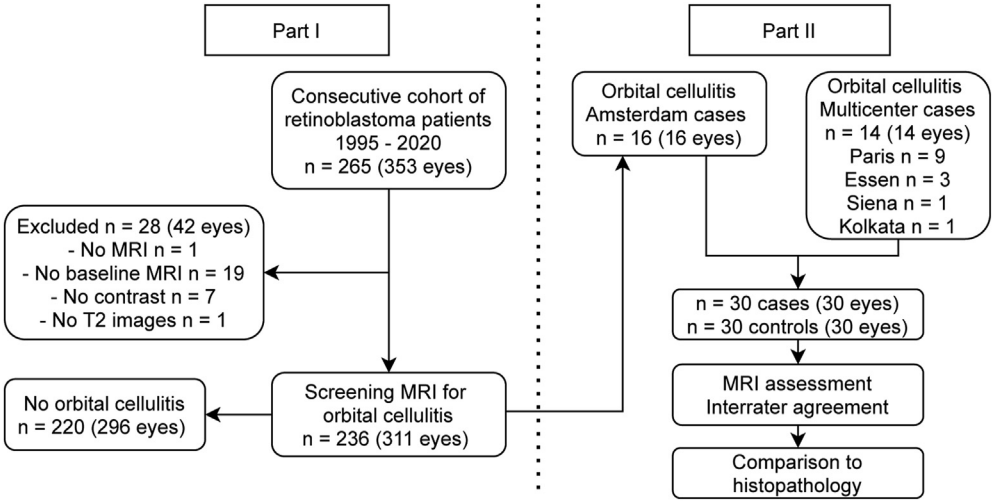


**Figure 1.** Flowchart of this combined study with a retrospective consecutive single-center part and a multicenter case–control part. MRI = magnetic resonance imaging.

through chart review or reexamination of material (sections or digital pictures).

### Statistical Analysis

Interreader agreement was calculated using Cohen's kappa or Fleiss' kappa. Associations between imaging features and diagnosis (orbital cellulitis vs. controls) were assessed using exact tests. The Bonferroni method was adopted to adjust *P* values for multiple testing. Bonferroni-adjusted *P* values below 0.05 were considered to be statistically significant. SPSS, version 26, was used to perform statistical analyses.

## Results

### Part I: Screening MRI Scans on Orbital Inflammatory Features

In the consecutive cohort, 265 patients and 353 retinoblastoma eyes were assessed (Fig 1). After adoption of exclusion criteria, 236 patients (311 eyes) were screened on the presence of retinoblastoma-associated orbital cellulitis. Prevalence of retinoblastoma-associated orbital cellulitis on MRI was 6.8% (16/236; 95% confidence interval [CI], 3.9–10.8). In 16 of 16 cases (100%) with orbital cellulitis on imaging (≥ 2 inflammatory features), orbital cellulitis diagnosis was confirmed by ophthalmic records. Table S1 (available at www.aaojournal.org) shows the frequency and interreader agreement of the inflammatory features on imaging. Figure 3 shows example MRI scans of 3 retinoblastoma-associated orbital cellulitis cases, representing all inflammatory features.

### Part II: MRI of Retinoblastoma-Associated Cellulitis Cases: Patient Characteristics

In total, 30 orbital cellulitis cases and 30 matched controls were identified (Fig 1, part II). Patient characteristics are available in Table 1. Clinical symptoms at presentation included warm, red, and swollen eyelids, hyperemia, proptosis, chemosis, high intraocular pressure, buphthalmos, or nausea. All retinoblastoma-associated orbital cellulitis cases were staged as International Classification of Retinoblastoma group E eyes and underwent enucleation. Three of 30 orbital cellulitis cases (10%) received preenucleation steroid treatment. Preenucleation chemotherapy was given to 17% (10/60) of patients in 27% (8/30) of orbital cellulitis patients and in 7% (2/30) of controls ($P = 0.08$).

### Inflammatory Features on MRI in Retinoblastoma-Associated Cellulitis

The frequency and interreader agreement (Kappa range, 0.40–1.00) of inflammation features are shown in Table 2. Preseptal inflammation (23/30, [77%]), postseptal inflammation (21/30, [70%]), and inflammation of the lacrimal gland (22/30, [73%]) were common features in orbital cellulitis cases ($P < 0.001$, Fig 3). Proptosis was more frequent in the orbital cellulitis group (12/30 [40%]) than in the control group (0/30 [0%]). Ninety-two percent of proptosis cases (11/12) showed postseptal orbital inflammation. Extraocular muscle inflammation was relatively rare and not significantly more frequent in orbital cellulitis cases when directly compared with matched controls.

### Intraocular Imaging Features in Retinoblastoma with Orbital Cellulitis

The frequency of the intraocular imaging features that were statistically significantly associated with orbital cellulitis cases is shown in Table 3. Other comparisons including nonsignificant results are available in Table S2 (available at www.aaojournal.org), also including interreader agreement statistics for all intraocular imaging features. Figure 4 shows examples of these MRI characteristics. Retinoblastoma with orbital cellulitis was, compared with controls, more often globe filling (50% [15/30] vs. 10% [3/30], $P = 0.045$), showed a total detachment of the retina (97% [29/30] vs. 63% [19/30] $P = 0.047$), and had an increased eye size (buphthalmos) (70% [21/30] vs. 23% [7/30], $P = 0.012$). Of all buphthalmos cases, only 32% (9/28) showed proptosis. Tumors in orbital cellulitis cases showed extensive necrosis. In 77% (22/30) of orbital cellulitis cases, the tumor was predominantly necrotic (> 67% necrosis), and in 43% (13/30) the tumor was near-totally necrotic (95%–100% of tumor), with absence of any contrast enhancement of the intraocular tumor as a consequence. Less than 67% necrosis was found in all of the controls ($P = 0.001$). Uveal necrosis and uveal

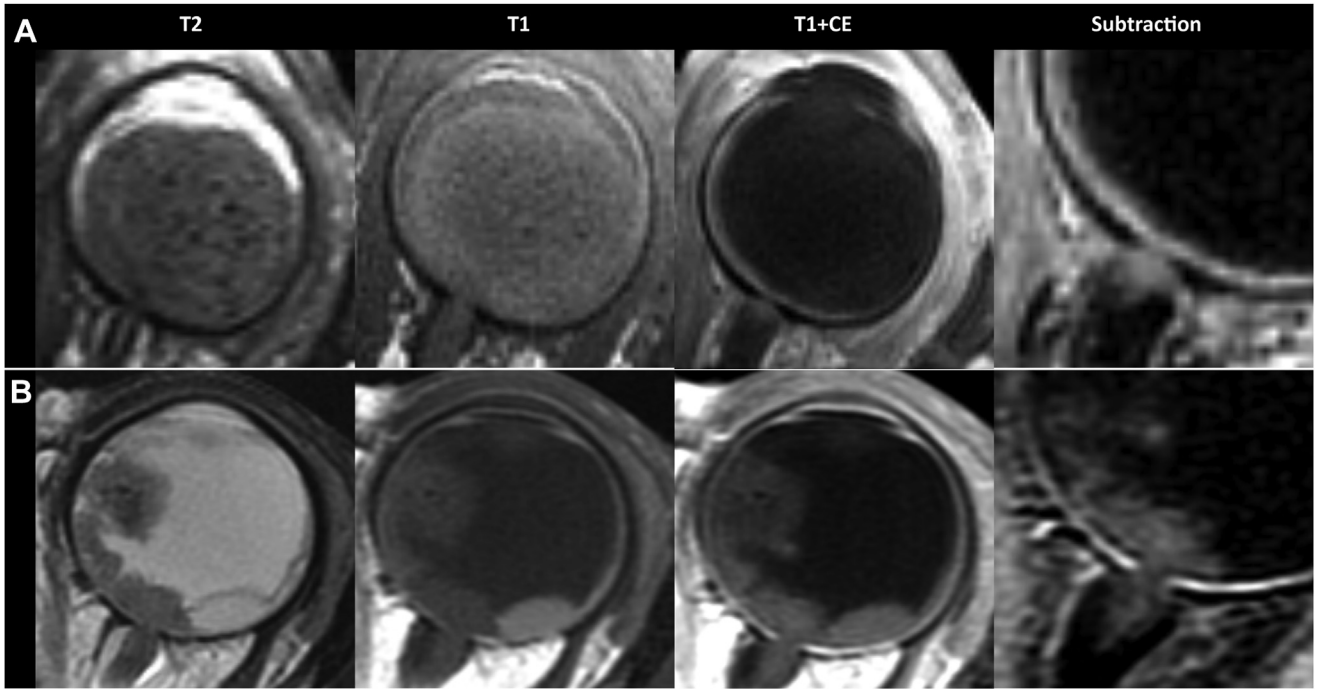


**Figure 2.** Examples of the 2 different patterns of postlaminar optic nerve enhancement (PLONE). **A,** Inflammatory PLONE, defined as a strong enhancement (equal to or greater in signal intensity than choroidal enhancement) in a rectangular shape covering the whole superficial width of the lamina cribrosa and distal optic nerve. **B,** Tumor-invasive PLONE, defined as an enhancement pattern with a moderate enhancement (less intense than choroidal enhancement) in a triangular shape into the optic nerve, with an interruption of the linear choroidal enhancement (reuse of previously published images in different context with permission of publisher[20]).

hemorrhage were both exclusively present in the orbital cellulitis group (70% [21/30] and 59% [17/29], respectively, $P < 0.001$). Uveal necrosis and uveal hemorrhage were located predominantly within the iris or ciliary body. In orbital cellulitis cases, uveitis (90% [27/30] vs. 10% [3/30]) and dislocated eye lens (63% [19/30] vs. 0% [0/30]) were more often present ($P = 0.001$). Tumor volume did not statistically significantly differ between cases and controls (1630 $mm^3$ vs. 1262 $mm^3$, $P = 0.68$).

### Detecting PLONI on MRI in Retinoblastoma with Orbital Cellulitis

Conventional methods for detecting PLONI on MRI comprise evaluation of PLONE and optic nerve enlargement, either present or absent. Examples of the more specific inflammatory enhancement pattern PLONE versus tumor invasion enhancement pattern PLONE are shown in Figure 2. In this study, 67% (20/30) of orbital cellulitis cases showed PLONE, 13% (4/30) showed invasive pattern PLONE, and 53% (16/30) showed inflammatory pattern PLONE (Table 4). Kappa values for interreader agreement for PLONE (present vs. absent) were 0.53 for comparisons between study reviewers and 0.66 for comparisons between consensus study read and clinical read (for 37 available clinical reads). Interreader agreement of specific PLONE patterns was 0.74. Adopting the conventional method for PLONI detection on MRI (PLONE present vs. PLONE absent) resulted in a specificity of 32% in orbital cellulitis cases (Table 4A). Inflammatory enhancement pattern in the optic nerve was found in 16 of 20 (80%) orbital cellulitis cases with optic nerve enhancement, of which 0 of 16 (0%) showed tumor invasion on histopathology. When combining inflammatory PLONE with absent PLONE as the low-risk category in PLONI prediction, specificity increased from 32% (95% CI, 16–52) to 89% (95% CI, 72–98) (Table 4B). The specificity of the control group remained the same when considering inflammatory PLONE as low risk for PLONI (Table 4B) because all PLONE found in the control cases was tumor-invasive PLONE. Figure 5 shows radiology-pathology correlations of both inflammatory PLONE pattern correlating to inflammation on histology and tumor-invasive pattern PLONE correlating to tumor cells within the optic nerve (Fig 5B: reuse of previously published images in different context with permission of publisher[22]). For sensitivity calculations, the CIs were large because of the low amount of PLONI cases within the orbital cellulitis group (Table 4). The single case of orbital cellulitis with PLONI showed PLONE with the tumor invasion pattern. Table 5 shows the 20 orbital cellulitis cases with PLONE, showing the length of PLONE, enhancement pattern, histopathology, and outcome after follow-up. Of the 16 cases with exclusively inflammatory pattern PLONE, 4 (25%) were treated with chemotherapy before enucleation, and 14 (88%) were alive without disease. One case (6%, 1/16) developed trilateral retinoblastoma (pineoblastoma) with subsequent leptomeningeal metastases and death, and 1 case (6% 1/16) was alive with intraocular disease in the contralateral eye. Table 5 also shows the only 2 cases with optic nerve enlargement (2/60, 3%), which were both orbital cellulitis cases, and both did not show PLONI on histopathology. However, both patients received neoadjuvant chemotherapy before enucleation.

## Discussion

The MRI phenotype of retinoblastoma with orbital cellulitis consists of significantly increased eye size, more tumor necrosis, uveal abnormalities (inflammation, hemorrhage,

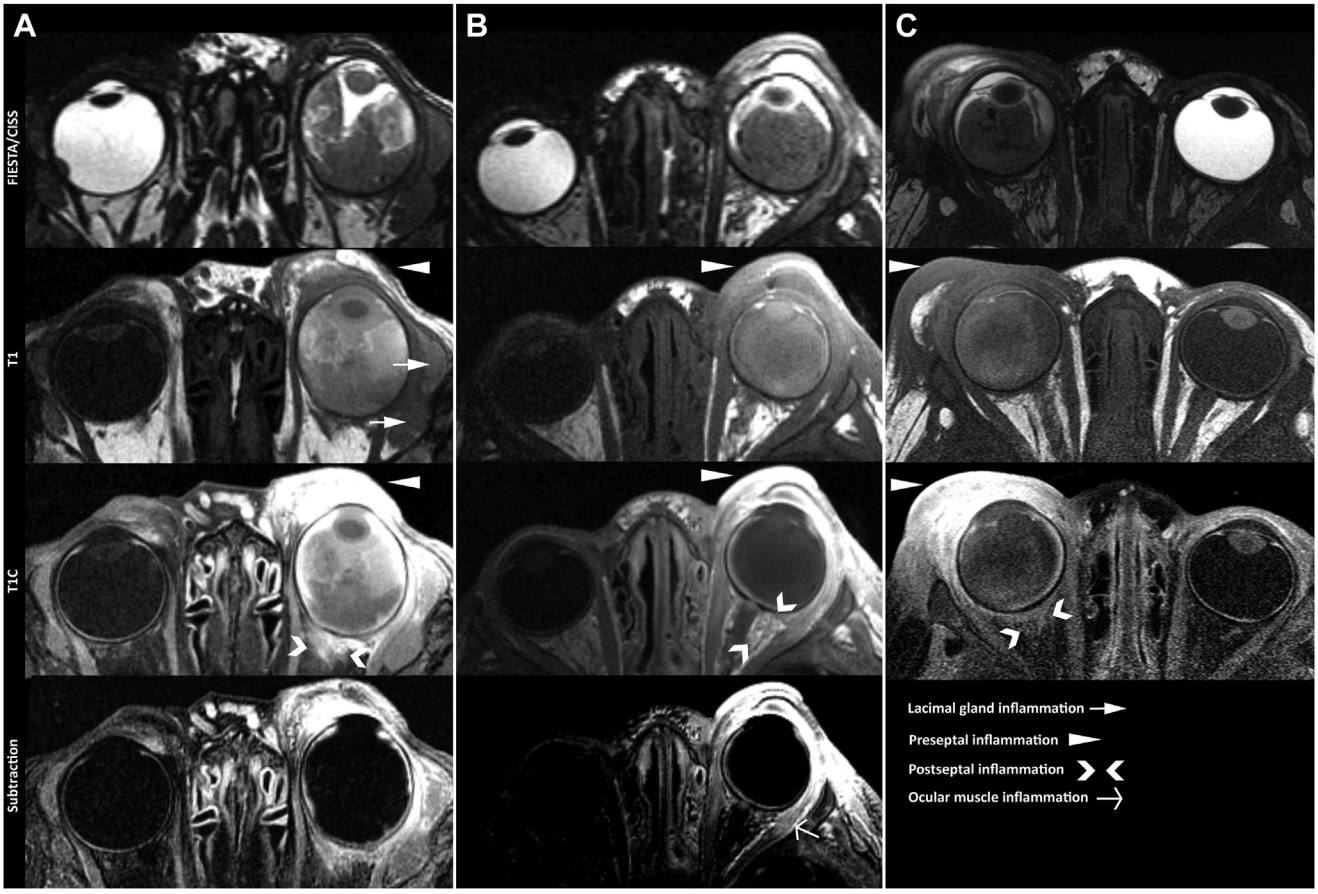


**Figure 3.** Inflammatory findings in retinoblastoma-associated orbital cellulitis in three individual patients (patient **A**, **B**, **C**): lacrimal gland inflammation, preseptal inflammation, postseptal inflammation, and ocular muscle inflammation. Proptotis (eye protrosion) associated with postseptal inflammation is present in patient **B**. Buphthalmos (enlarged eye size vs. contralateral eye; patient **A** and **B**) is also displayed as an intraorbital finding of retinoblastoma-associated orbital cellulitis.

and necrosis), and lens luxation. By adopting patterns of enhancement within the optic nerve, distinction of optic nerve inflammation from tumor invasion could be improved for retinoblastoma with orbital cellulitis.

Magnetic resonance imaging is incorporated in standard-of-care pretreatment evaluation of retinoblastoma in most high-income countries for examining disease extent, screening central nervous system for metastasis and trilateral

Table 1. Patient Characteristics

| | Total | Orbital Cellulitis Cases | Controls | *P* Value |
|---|---|---|---|---|
| N patients (1 eye per patient included), n (%) | 60 | 30 (50) | 30 (50) | 1 |
| Female sex, n (%) | 28 (47%) | 16 (53) | 12 (40) | 0.44* |
| Median age at scandate (mos), n (range) | 16 (0–59) | 12 (0–59) | 19 (0–53) | 0.08† |
| Clinical diagnosis of orbital cellulitis, n (%) | 30 (50%) | 30 (100) | 0 (0) | |
| International Classification of Retinoblastoma, n (%) | | | | 0.001* |
| A/B/C | 0 (0) | 0 (0) | 0 (0) | |
| D | 10 (17) | 0 (0) | 10 (33) | |
| E | 50 (83) | 30 (100) | 20 (67) | |
| Enucleation of the eye, n (%) | 60 (100) | 30 (100) | 30 (100) | 1 |
| Patients with bilateral disease, n (%) | 25 (42) | 16 (53) | 9 (30) | 0.12* |
| Hereditary retinoblastoma, n (%)‡ | 18/46 (39) | 14/26 (54) | 4/20 (20) | 0.32* |
| Preenucleation chemotherapy | 10 (17%) | 8 (27%) | 2 (7%) | 0.08* |
| Preenucleation steroid therapy | 3 (5%) | 3 (10%) | 0 (0%) | 0.24* |

**P* values based on Fisher exact test. †*P* values based on independent sample *t* test.
‡Data available for n = 46 patients.

Table 2. Orbital Cellulitis MRI Inflammation Features

| MRI Feature | Orbital Cellulitis Cases (N = 30) | Controls (N = 30) | Total (N = 60) | *P* Value* | Interreader Agreement (Kappa) |
|---|---|---|---|---|---|
| Preseptal orbital inflammation, n (%) | 23 (77) | 1 (7) | 25 (42) | **<0.001** | 0.73 |
| Proptosis, n (%) | 12 (40) | 0 (0) | 12 (20) | **<0.001** | 0.76 |
| Postseptal orbital inflammation, n (%) | 21 (70) | 2 (7) | 23 (38) | **<0.001** | 0.40 |
| Inflammation of extraocular muscles, n (%) | 6 (20) | 0 (0) | 6 (10) | 0.12 | 0.84 |
| Inflammation of the lacrimal gland, n (%) | 22 (73) | 1 (3) | 23 (38) | **<0.001** | 1.00 |

MRI = magnetic resonance imaging.
**P* values were derived from Fisher exact tests adopting Bonferroni correction for multiple testing; significant results are in bold.

disease, and supporting the diagnosis. In context of orbital cellulitis, the diagnosis of retinoblastoma may be challenging, considering other conditions in the differential diagnosis such as uveitis, scleritis, panophthalmitis, or orbital cellulitis without retinoblastoma.[17] Traits on MRI suggesting retinoblastoma as the underlying condition for the orbital cellulitis are a T2-hypointense intraocular mass that is predominantly necrotic (nonenhancing tumor mass) with calcifications and is frequently combined with lens luxation and a strong uveal enhancement. Additionally, MRI is used in retinoblastoma care for examining risk factors for metastasis and local recurrence, with the most frequent risk factors being massive choroidal invasion (8%–15%) and PLONI (10%–20%),[4,23,24] of which the latter was investigated in this study in the context of orbital cellulitis.

The prevalence in this study of retinoblastoma-associated orbital cellulitis (6.8%) was comparable to previous reports (4.8%–5.4%).[11,12] Intraocular features in cases of retinoblastoma-associated orbital cellulitis are concordant with findings in smaller case series[10,11,17] and support the hypothesis that retinoblastoma-associated cellulitis is caused by auto-infarction and necrosis, with necrotic products causing sterile inflammation.[11] The necrosis is probably caused by either the tumor outgrowing its blood supply or a high intraocular pressure causing central retinal artery occlusion or venous congestion. The MRI phenotype matched with this hypothesis, with extensive intratumoral necrosis being present in all cellulitis cases. The high frequency of globe-filling or retina-filling tumors combined with a young age at diagnosis supports the fast tumor growth. The frequently found total retinal detachments may play a role in ischemia through subsequent obstruction of intratumoral blood supply. The high frequency of buphthalmos supports high intraocular pressure, with possible subsequent central retinal artery occlusion or venous congestion. Surprisingly, tumor volume was not

Table 3. Intraocular Imaging Features Associated with Orbital Cellulitis

| MRI Feature | Scores | Cases (N = 30) | Controls (N = 30) | Total (N = 60) | *P* Value |
|---|---|---|---|---|---|
| Greater eye size (buphthalmos) | | 70% (21/30) | 23% (7/30) | 47% (28/60) | 0.012† |
| Tumor location | | | | | 0.045* |
| | Greater part of tumor in front of equator | 3% (1) | 0% (0) | 2% (1) | |
| | Greater part of tumor behind equator | 37% (11) | 67% (20) | 52% (31) | |
| | Entire globe filled | 50% (15) | 10% (3) | 30% (18) | |
| | Entire retina filled | 10% (3) | 23% (7) | 17% (10) | |
| Retinal detachment | | | | | 0.047† |
| | No detachment | 0% (0) | 0% (0) | 0% (0) | |
| | Partial detachment | 3% (1) | 37% (11) | 20% (12) | |
| | Total detachment | 97% (29) | 63% (19) | 80% (48) | |
| Proportion contrast-enhancing tumor | | | | | <0.001‡ |
| | <33% | 77% (23) | 0% (0) | 38% (23) | |
| | 34%–67% | 17% (5) | 37% (11) | 27% (16) | |
| | >68% | 7% (2) | 63% (19) | 35% (21) | |
| Proportion necrotic tumor | | | | | <0.001‡ |
| | <33% | 7% (2) | 67% (20) | 37% (22) | |
| | 34%–67% | 17% (23) | 33% (10) | 25% (15) | |
| | >68% | 77% (23) | 0% (0) | 38% (23) | |
| Uveitis (choroidal thickening) | | 90% (27) | 10% (3) | 50% (30) | <0.001† |
| Uveal necrosis | | 70% (21) | 0% (0) | 35% (21) | <0.001† |
| Uveal hemorrhage§ | | 59% (17) | 0% (0) | 29% (17) | <0.001† |
| Dislocated eye lens | | 63% (19) | 0% (0) | 0% (0) | <0.001† |

**P* values were derived from Fisher-Freeman-Halton tests adopting Bonferroni correction for multiple testing. †*P* values were derived from Fisher exact tests, adopting Bonferroni correction for multiple testing. ‡*P* values were derived from chi-square trend tests, adopting Bonferroni correction for multiple testing.
§Percentages based on n = 29 cases and n = 29 controls because n = 2 were scored as indeterminate.

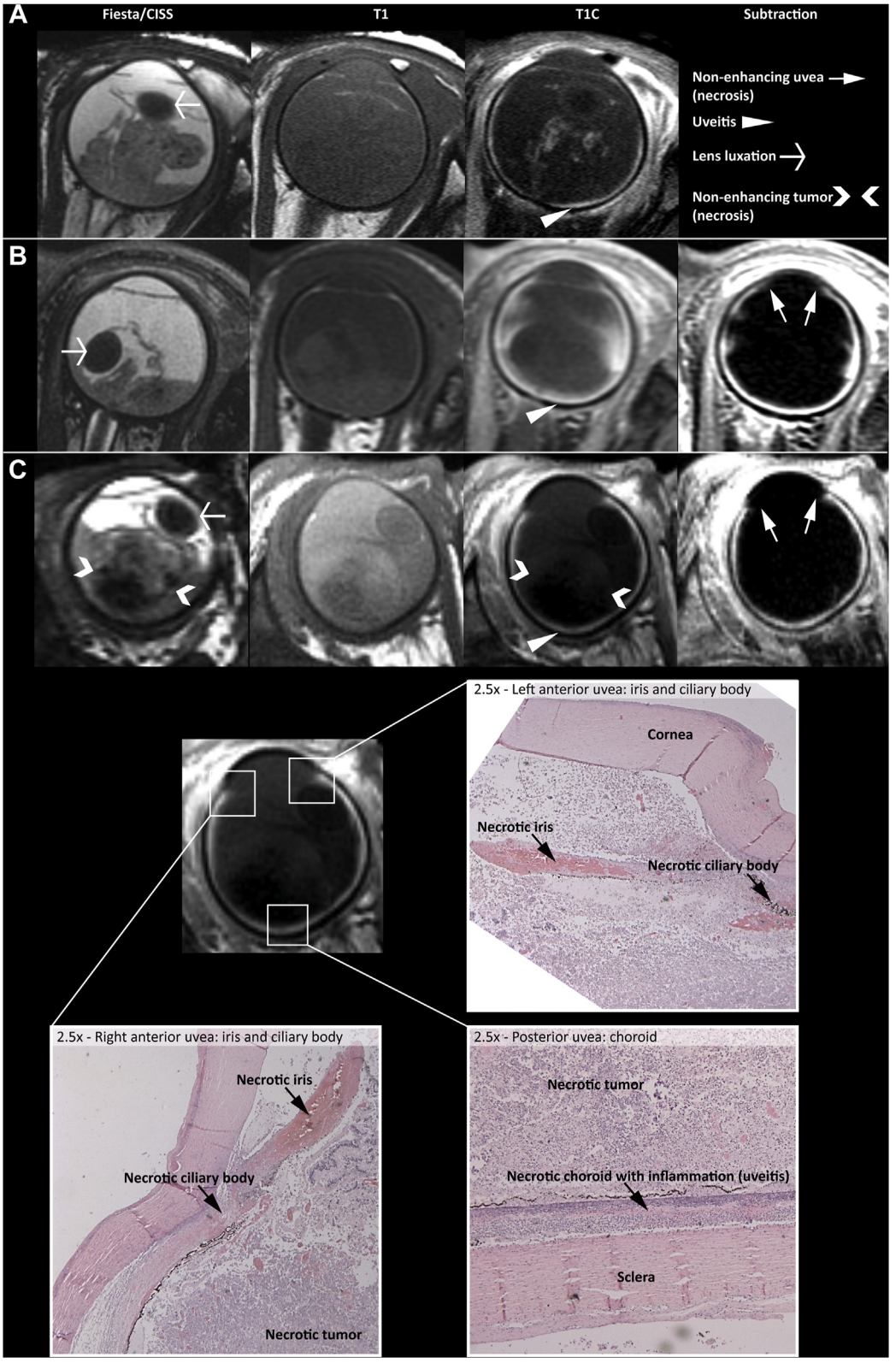


**Figure 4.** Intraorbital findings of retinoblastoma with orbital cellulitis. **A and B,** Magnetic resonance imaging (MRI) shows lens luxation, extensive necrosis of the tumor (>95%, tumors with heterogeneous signal intensity without contrast enhancement), uveitis (choroidal thickening with strong enhancement), and uveal necrosis of the ciliary body (no enhancement of ciliary body). **C,** The MRI histopathological correlation of a retinoblastoma patient with orbital cellulitis, with histopathology showing extensive tumor necrosis, necrosis in all uvea areas (bilateral ciliary body and iris, choroid), and choroidal inflammation (uveitis).

Table 4. Diagnostic Accuracy of PLONE for Predicting Metastatic Risk Factor PLONI

**Test A: Assessing PLONE Presence without Considering PLONE Patterns**
Considering Presence of PLONE High Risk and Absence of PLONE Low Risk for PLONI

| | *Orbital Cellulitis Cases* | | *Controls* | |
|---|---|---|---|---|
| | *PLONI+* | *PLONI-* | *PLONI+* | *PLONI-* |
| PLONE present | 1 | 19 | 4 | 2 |
| PLONE absent | 0 | 9 | 5 | 19 |
| Sensitivity (CI) | 100% (3–100) | | 44% (14–78) | |
| Specificity (CI) | 32% (16–52) | | 90% (70–99) | |

**Test B: Assessing PLONE Considering PLONE Enhancement Patterns**
Considering Solely PLONE with Invasive Pattern as High Risk for PLONI and Either Inflammatory Pattern PLONE or Absent PLONE as Low Risk for PLONI

| | *Orbital Cellulitis Cases** | | *Controls* | |
|---|---|---|---|---|
| | *PLONI+* | *PLONI-* | *PLONI+* | *PLONI-* |
| Invasive PLONE present | 1 | 3 | 4 | 2 |
| Invasive PLONE absent (inflammatory PLONE present/PLONE absent) | 0 (0/0) | 25 (16/9) | 5 (0/5) | 19 (0/19) |
| Sensitivity (CI) | 100% (3%–100%) | | 44% (14%–78%) | |
| Specificity (CI) | 89% (72%–98%) | | 90% (70%–99%) | |

CI = confidence interval; PLONE = postlaminar optic nerve enhancement; PLONI = postlaminar optic nerve invasion.
*One orbital cellulitis case (1/30, 3%) was excluded from analysis because histopathologic data were missing.

significantly larger in orbital cellulitis cases in the current study, possibly because of the selection of enucleated controls, which are generally of a more advanced stage, and the selection of PLONI patients within the control group, which on average have larger tumor volume.[4] It is also suggested that a necrotic ciliary body and iris cause an inflammatory response in the adjacent orbital tissues by leakage of necrotic products through the trabecular channels.[12] Correspondingly, in our MRI study, the ciliary body and iris were often affected. The luxation of the lens is likely to be the result of ciliary body necrosis, which supports the suspensory ligaments of the lens. Without interpreting PLONE patterns, PLONE was an unreliable predictor of PLONI in the context of orbital cellulitis. The specificity of PLONE found in orbital cellulitis cases (32%) was lower than in retinoblastoma patients without orbital cellulitis in recent systematic reviews (88%–94%).[5,25] The amount of false-positive PLONE is higher in the case of retinoblastoma-associated orbital cellulitis in our study than in the general retinoblastoma population (19/29 [66%] vs. 53/97 [55%], respectively).[5] This false-positive PLONE is probably caused by an extension of inflammation from the choroid into the adjacent optic nerve disc and may also account for a part of the false-positives in the general retinoblastoma population. Optic nerve enlargement was an unreliable predictor of PLONI in this study. The only 2 cases with this finding also showed extensive PLONE of the invasive pattern but did not show PLONI on histopathologic evaluation. However, both cases received neoadjuvant chemotherapy before enucleation (cases 22 and 24, Table 5), possibly leading to unreliable histopathologic results clarifying the poor performance of optic nerve enlargement as a predictor of PLONI in our relatively small series of patients. However, the exact reliability of histopathologic risk factors after neoadjuvant treatment remains uncertain.[6,26-28]

The results of this study confirmed the findings of 4 previously published MRI cases,[10] indicating that PLONE probably can be caused by inflammation, tumor invasion, or both simultaneously. Inflammatory enhancement was defined as equal or greater signal intensity than choroidal enhancement covering the whole superficial width of the lamina cribrosa and distal optic nerve. According to the results of this study, the presence of inflammatory enhancement will lead to an unlikely diagnosis of tumor within the optic nerve. From a pathophysiological perspective, the intraocular inflammatory reaction may be due to leakage of necrotic tumor products, leading to choroidal inflammation that extends into the adjacent optic nerve fibers within the lamina cribrosa. This may explain the broad pattern of PLONE of the whole superficial width of the optic nerve, with inflammation-induced vessel dilatation and vascular leakage with strong contrast enhancement as a result. This enhancement is isointense compared with the inflamed choroid. In contrast, the tumor-invasive PLONE pattern follows the spread of invasive retinoblastoma tumor cells into the optic nerve, usually triangularly in shape with or without a full-width connection to the adjacent choroid, showing an isointense enhancement with respect to the intraocular tumor, which is always less intense than the choroid. Steroid administration appeared to be rare for this type of sterile cellulitis among participating centers, in only 10% of cases, probably because of the advanced stage of these tumors, generally treated with prompt enucleation.

By interpreting inflammatory pattern PLONE as low risk for PLONI, regarding only invasive pattern PLONE as high risk for PLONI, the number of false-positives decreased

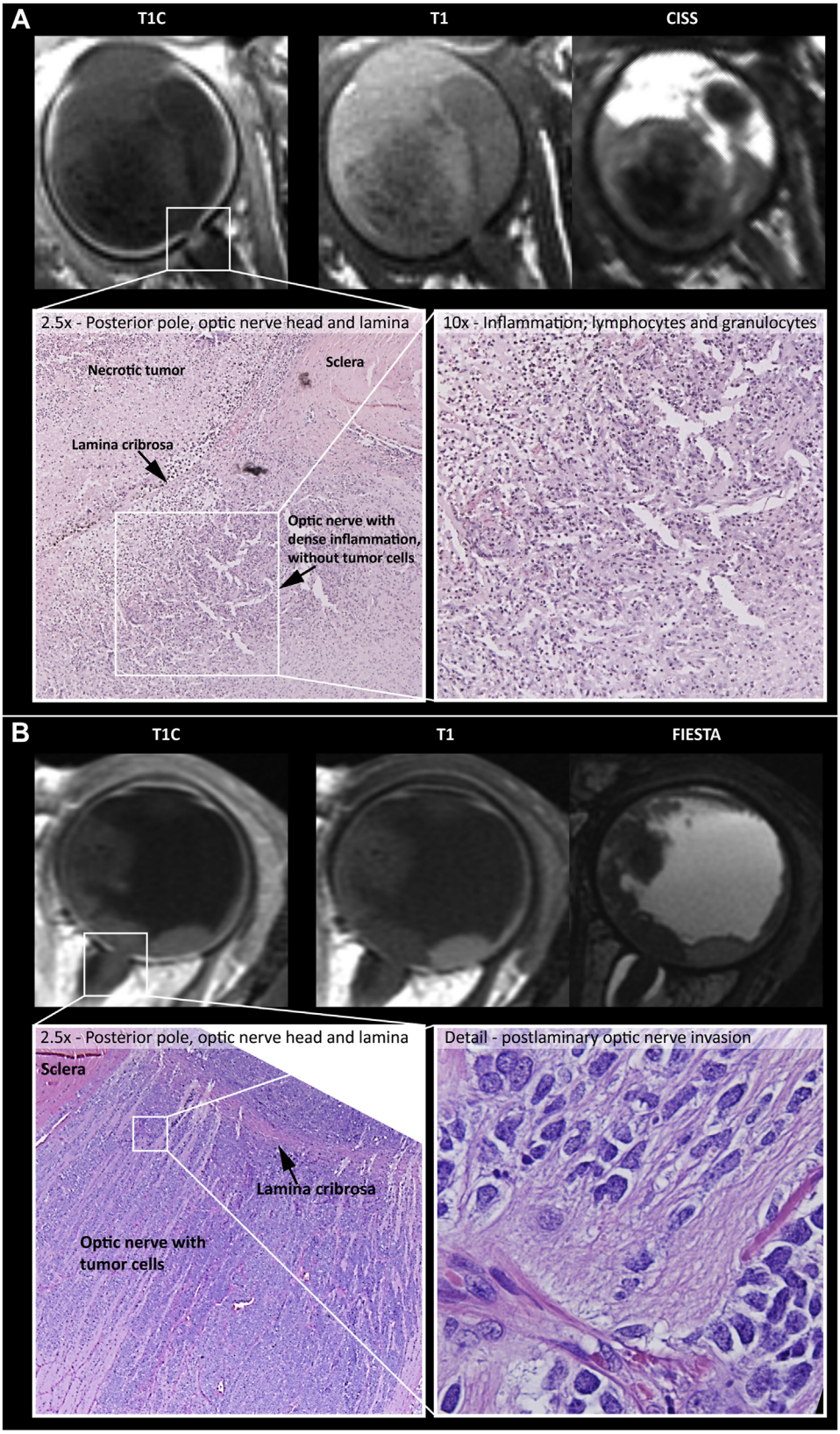


**Figure 5.** The magnetic resonance imaging (MRI)-pathological correlations of postlaminar optic nerve enhancement (PLONE) tab patterns. **A,** Inflammation pattern PLONE with no postlaminar optic nerve invasion (PLONI) on histopathology assessment. **B,** Invasion pattern PLONE with PLONI on histopathology assessment (reuse of previously published images in different context with permission of publisher[20]).

Table 5. MRI, Histopathology, and Clinical Outcome of 20 Orbital Cellulitis Cases with PLONE

| Case | Sex | Age (mos) | Length of PLONE on MRI (mm) | Tumor Connected to Optic Disc | Optic Nerve Enlargement | Enhancement Pattern | PLONI on Histopathology | Preenucleation Chemotherapy | Outcome* |
|---|---|---|---|---|---|---|---|---|---|
| 1 | M | 1 | 1.1 | Yes | No | Inflammatory | No | No | Alive without disease |
| 2 | M | 4 | 1.6 | No | No | Inflammatory | No | No | Alive without disease |
| 3 | M | 2 | 3.1 | Yes | No | Inflammatory | No | No | Death, pineoblastoma with leptomeningeal metastasis |
| 4 | M | 4 | 1.7 | Yes | No | Inflammatory | No | No | Alive without disease |
| 6 | F | 27 | 3.0 | Yes | No | Inflammatory | No | No | Alive without disease |
| 7 | F | 2 | 1.7 | No | No | Inflammatory | No | No | Alive without disease |
| 8 | M | 0 | 0.9 | No | No | Inflammatory | No | No | Alive without disease |
| 9 | M | 13 | 1.2 | Yes | No | Inflammatory | No | No | Alive without disease |
| 10 | M | 15 | 1.1 | Yes | No | Inflammatory | No | No | Alive without disease |
| 11 | M | 22 | 1.5 | Yes | No | Inflammatory | No | No | Alive without disease |
| 15 | F | 30 | 2.1 | Yes | No | Inflammatory | No | NA | Alive without disease |
| 17 | F | 0 | 0.7 | Yes | No | Inflammatory | No | No | Alive with local intraocular disease |
| 19 | M | 11 | 1.4 | Yes | No | Inflammatory | No | 1 cycle VP-Ca | Alive without disease |
| 21 | F | 1 | 1.9 | Yes | No | Inflammatory | No | 1 cycle VP-Ca | Alive without disease |
| 23 | M | 11 | 1.3 | Yes | No | Inflammatory | No | 3 cycles VP-Ca-Vi | Alive without disease |
| 26 | F | 1 | 1.5 | Yes | No | Inflammatory | No | 1 cycle VP-Ca | Alive without disease |
| 5 | M | 49 | 4.2 | Yes | No | Tumor invasive† | Yes | No | Death, local relapse with leptomeningeal metastasis |
| 24 | M | 29 | 20.7‡ | Yes | Yes | Tumor invasive† | No | 3 cycles VP-Ca-Vi-Th | Alive without disease |
| 16 | F | 3 | 1 | No | No | Tumor invasive | No | No | Alive with local intraocular disease |
| 22 | F | 59 | 22‡ | Yes | Yes | Tumor invasive | No | 3 cycles VP-Ca-Vi-Th | Alive without disease |

Ca = carboplatin; Et = etoposide; MRI = magnetic resonance imaging; NA = not available; PLONE = postlaminar optic nerve enhancement; PLONI = postlaminar optic nerve invasion; Th = intrathecal thiotepa; Vi = vincristine; VP = VP-16.
*In case of "alive without disease," no metastasis developed.
†Two cases with both tumor-invasive pattern and inflammatory pattern PLONE were interpreted as tumor-invasive pattern PLONE.
‡Two cases with high suspicion of PLONI on MRI with both extensive PLONE on contrast-enhanced sequences and radiological appearance of tumor invasion on other sequences including optic nerve enlargement had no PLONI on histopathology after enucleation, possibly because they were treated extensively with chemotherapy before enucleation.

significantly. The amount of PLONI cases and the current study design were not adequate for drawing conclusions on the positive predictive value. Nonetheless, the knowledge that PLONE can be caused by inflammation and the defined characteristics of inflammatory and tumor-invasive PLONE are relevant clinically for tailoring treatment based on the predicted presence or absence of PLONI. Although retinoblastoma with orbital cellulitis generally presents as advanced stage disease and therefore generally requires enucleation, it is still important to interpret PLONE correctly because it enables clinicians to refine the treatment regimen. When risk for PLONI can be more accurately estimated on pretreatment imaging, for low-risk cases, clinicians could refrain from neoadjuvant chemotherapy before enucleation or omit an extended dissection of the optic nerve during enucleation,[29] a procedure that is already challenging technically in the presence of extensive inflammation in orbital cellulitis. In some of these orbital cases, however, severe buphthalmos may be an independent reason to include neoadjuvant chemotherapy (to avoid globe rupture) and to enucleate regardless of PLONE interpretation. Nonetheless, the field of application of eye-sparing treatment methods is growing, also in advanced retinoblastoma cases.[7,8] With a lack of histopathologic evaluation in these cases, MRI interpretation of PLONE may become increasingly important for tailoring therapy. In addition, as discussed, for patients who received preenucleation chemotherapy, histopathologic results for extraocular extension may be unreliable, augmenting the importance of correct imaging-based classification of these cases.[6,26-28]

## Study Limitations

This study yielded several limitations. It was a retrospective study, and although the described cohort is large compared with others available in the literature, the cohort was limited in size, resulting in large CIs. Moreover, clinical details of the cohort of part I of this study were not complete enough to assess the amount of clinical orbital cellulitis cases that might be missed in radiological review (false-negative MRI). Likewise, the study design was only aimed at investigating retinoblastoma-associated orbital cellulitis and the risk factor PLONI, which left other risk factors such as choroidal invasion beyond the scope of this article. Furthermore, comparisons of PLONE before and after steroid administration may be of interest for future studies, as may comparing PLONE in retinoblastoma versus

nonretinoblastoma cellulitis cases, but the amount of cases was insufficient to evaluate these topics in the current study. Finally, the interreader agreement varied extensively between MRI features, possibly in part because of the novelty of some imaging features or the required spatial resolution to assess the imaging features. However, interreader agreement on optic nerve enhancement and enhancement patterns was relatively high, indicating they can be useful in clinical practice.

## Conclusions

Retinoblastoma cases presenting with orbital cellulitis show MRI findings of a larger eye size, extensive tumor necrosis, uveal abnormalities, and lens luxation. Magnetic resonance imaging contrast-enhancement patterns within the postlaminar optic nerve can differentiate between tumor invasion and inflammatory changes and thereby improve metastatic risk stratification.

## Footnotes and Disclosures

Originally received: December 31, 2021.
Final revision: May 31, 2022.
Accepted: June 13, 2022.
Available online: June 22, 2022. Manuscript no. OPHTHA-D-21-02502.

[1] Department of Radiology and Nuclear Medicine, Amsterdam UMC, Vrije Universiteit Amsterdam, Cancer Center Amsterdam, Amsterdam, The Netherlands.

[2] European Retinoblastoma Imaging Collaboration.

[3] Department of Radiology, Institut Curie, Paris, France.

[4] Paris University, Paris, France.

[5] Department of Diagnostic and Interventional Radiology and Neuroradiology, University Hospital Essen, Essen, Germany.

[6] Department of Neuroimaging and Neurointervention, Siena University Hospital, Siena, Italy.

[7] Department of Radiology, Centre Hospitalier Universitaire Vaudois and University of Lausanne, Lausanne, Switzerland.

[8] Department of Radiology and Imaging Sciences, Tata Medical Center, Kolkata, India.

[9] Department of Ophthalmology, University Hospital Essen, Essen, Germany.

[10] Department of Ophthalmology, Amsterdam UMC, Vrije Universiteit Amsterdam, Cancer Center Amsterdam, Amsterdam, The Netherlands.

[11] Department of Pathology, Amsterdam UMC, Vrije Universiteit Amsterdam, Cancer Center Amsterdam, Amsterdam, The Netherlands.

*Members of the European Retinoblastoma Imaging Collaboration appear in the Appendix (available at www.aaojournal.org).

Disclosure(s):

All authors have completed and submitted the ICMJE disclosures form.

The author(s) have no proprietary or commercial interest in any materials discussed in this article.

This study has received funding by Stichting Kinderen Kankervrij (KIKA), Grant Number 342 and by the Hanarth Foundation, Grant for project titled *MRI-based Deep Learning Segmentation and Quantitative Radiomics in Retinoblastoma: A Next Step Towards Personalized Interventions.* The sponsors or funding organizations had no role in the design or conduct of this research.

Results of this study were presented at: the International Society for Genetic Eye Diseases and Retinoblastoma Meeting, Lausanne, Switzerland, September 3, 2021.

HUMAN SUBJECTS: Human subjects were included in this study. Institutional Review Board (IRB)/Ethics Committee approval was obtained with waiver of informed consent. All research adhered to the tenets of the Declaration of Helsinki.

No animal subjects were used in this study.

Author Contributions:

Conception and design: Jansen, Sirin, Galluzzi, Göricke, Brisse, Maeder, Castelijns, Moll, de Jong, de Graaf

Data collection: Jansen, van der Heide, Cardoen, Sirin, de Bloeme, Galluzzi, Göricke, Brisse, Maeder, Sen, Biewald, Moll, van der Valk, de Jong, de Graaf

Analysis and interpretation: Jansen, van der Heide, Cardoen, Sirin, de Bloeme, Galluzzi, Göricke, Brisse, Maeder, Sen, Biewald, Castelijns, Moll, van der Valk, de Jong, de Graaf

Obtained funding: Jansen, de Jong, de Graaf

Overall responsibility: Jansen, van der Heide, Cardoen, Sirin, de Bloeme, Galluzzi, Göricke, Brisse, Maeder, Biewald, Castelijns, Moll, van der Valk, de Jong, de Graaf

Abbreviations and Acronyms:
**CI** = confidence interval; **MRI** = magnetic resonance imaging; **PLONE** = postlaminar optic nerve enhancement; **PLONI** = postlaminar optic nerve invasion.

Keywords:
Inflammation, Magnetic resonance imaging, Optic nerve, Orbital cellulitis, Retinoblastoma.

Correspondence:
Robin W. Jansen, MD, Department of Radiology and Nuclear Medicine, Amsterdam UMC, De Boelelaan 1117, 1081HV Amsterdam, The Netherlands. E-mail: r.jansen1@amsterdamumc.nl.

## References

1. Dimaras H, Kimani K, Dimba EA, et al. Retinoblastoma. *Lancet*. 2012;379:1436–1446.
2. Gündüz K, Müftüoglu O, Günalp I, et al. Metastatic retinoblastoma clinical features, treatment, and prognosis. *Ophthalmology*. 2006;113:1558–1566.
3. Brisse HJ, de Graaf P, Galluzzi P, et al. Assessment of early-stage optic nerve invasion in retinoblastoma using high-resolution 1.5 Tesla MRI with surface coils: a multicentre, prospective accuracy study with histopathological correlation. *Eur Radiol*. 2015;25:1443–1452.
4. De Jong MC, van der Meer FJ, Goricke SL, et al. Diagnostic accuracy of intraocular tumor size measured with MR imaging in the prediction of postlaminar optic nerve invasion and massive choroidal invasion of retinoblastoma. *Radiology*. 2016;279:817–826.
5. de Jong MC, de Graaf P, Noij DP, et al. Diagnostic performance of magnetic resonance imaging and computed tomography for advanced retinoblastoma: a systematic review and meta-analysis. *Ophthalmology*. 2014;121:1109–1118.

6. Choucair ML, Brisse HJ, Freneaux P, et al. Management of advanced uni- or bilateral retinoblastoma with macroscopic optic nerve invasion. *Pediatr Blood Cancer*. 2020;67:e27998.
7. Abramson DH, Gobin YP, Francis JH. Orbital retinoblastoma treated with intra-arterial chemotherapy. *Ophthalmology*. 2021;128:1437.
8. Zhou C, Wen X, Ding Y, et al. Eye-preserving therapies for advanced retinoblastoma: a multicenter cohort of 1678 patients in China. *Ophthalmology*. 2022;129:209–219.
9. Künkele A, Wilm J, Holdt M, et al. Neoadjuvant/adjuvant treatment of high-risk retinoblastoma: a report from the German Retinoblastoma Referral Centre. *Br J Ophthalmol*. 2015;99:949–953.
10. Chawla B, Duraipandi K, Sharma S. MRI in retinoblastoma with orbital cellulitis. *Ophthalmology*. 2013;120:1308–1309.e1-4.
11. Mullaney PB, Karcioglu ZA, Huaman AM, al-Mesfer S. Retinoblastoma associated orbital cellulitis. *Br J Ophthalmol*. 1998;82:517–521.
12. Walinjkar J, Krishnakumar S, Gopal L, et al. Retinoblastoma presenting with orbital cellulitis. *J AAPOS*. 2013;17:282–286.
13. Kaliki SJS, Vempuluru VS, Mallu A, Mishra DK. Retinoblastoma associated with orbital pseudocellulitis and high-risk retinoblastoma: a study of 32 eyes. *Int Ophthalmol*. 2022;42:19–26.
14. Foster BS, Mukai S. Intraocular retinoblastoma presenting as ocular and orbital inflammation. *Int Ophthalmol Clin*. 1996;36:153–160.
15. Shields JA, Shields CL, Suvarnamani C, et al. Retinoblastoma manifesting as orbital cellulitis. *Am J Ophthalmol*. 1991;112:442–449.
16. Nalci H, Gunduz K, Erden E. Necrotic intraocular retinoblastoma associated with orbital cellulitis. *Surv Ophthalmol*. 2018;63:114–118.
17. Pinto A, Puente Jr M, Shaikh F, et al. Aseptic pediatric orbital cellulitis: retinoblastoma until otherwise proven. *Ophthalmic Genet*. 2019;40:488–492.
18. Agarwal M, Biswas J, Krishnakumar S, Shanmugam MP. Retinoblastoma presenting as orbital cellulitis: report of four cases with a review of the literature. *Orbit*. 2004;23:93–98.
19. Suzuki S. A case of bilateral retinoblastoma with left orbital cellulitis. *Jpn J Clin Oncol*. 2009;39:274.
20. Bossuyt PM, Reitsma JB, Bruns DE, et al. STARD 2015: an updated list of essential items for reporting diagnostic accuracy studies. *Radiology*. 2015;277:826–832.
21. Jansen RW, de Jong MC, Kooi IE, et al. MR imaging features of retinoblastoma: association with gene expression profiles. *Radiology*. 2018;288:506–515.
22. de Jong MC, Van Der Valk P, Jansen RW, et al. Full-width postlaminar optic nerve tumor invasion of retinoblastoma as risk-factor for leptomeningeal spread of retinoblastoma. A case report and review of the literature. *Ophthalmic Genet*. 2020;41:69–72.
23. Khelfaoui F, Validire P, Auperin A, et al. Histopathologic risk factors in retinoblastoma: a retrospective study of 172 patients treated in a single institution. *Cancer*. 1996;77:1206–1213.
24. Eagle Jr RC. High-risk features and tumor differentiation in retinoblastoma: a retrospective histopathologic study. *Arch Pathol Lab Med*. 2009;133:1203–1209.
25. Cho SJ, Kim JH, Baik SH, et al. Diagnostic performance of MRI of postlaminar optic nerve invasion detection in retinoblastoma: a systematic review and meta-analysis. *Neuroradiology*. 2021;63:499–509.
26. Zhao J, Dimaras H, Massey C, et al. Pre-enucleation chemotherapy for eyes severely affected by retinoblastoma masks risk of tumor extension and increases death from metastasis. *J Clin Oncol*. 2011;29:845–851.
27. Chantada G, Leal-Leal C, Brisse H, et al. Is it pre-enucleation chemotherapy or delayed enucleation of severely involved eyes with intraocular retinoblastoma that risks extraocular dissemination and death? *J Clin Oncol*. 2011;29:3333–3334; author reply 5-6.
28. Eagle Jr RC, Shields CL, Bianciotto C, et al. Histopathologic observations after intra-arterial chemotherapy for retinoblastoma. *Arch Ophthalmol*. 2011;129:1416–1421.
29. Bellaton E, Bertozzi AI, Behar C, et al. Neoadjuvant chemotherapy for extensive unilateral retinoblastoma. *Br J Ophthalmol*. 2003;87:327–329.